Diffusion and thermalization in a boundary-driven dephasing model

Xhek Turkeshi [1,2,3,*] and Marco Schiró[4,†]

[1]*Scuola Internazionale Superiore di Studi Avanzati, Via Bonomea 265, 34136 Trieste, Italy*
[2]*Istituto Nazionale di Fisica Nucleare, Via Bonomea 265, 34136 Trieste, Italy*
[3]*The Abdus Salam International Centre for Theoretical Physics, Strada Costiera 11, 34151 Trieste, Italy*
[4]*Jeunes Équipes de l'Institut de Physique, USR 3573, Centre National de la Recherche Scientifique, Collége de France,*
PSL Research University, 11 Place Marcelin Berthelot, 75231 Paris Cedex 05, France

We study a model of noninteracting spinless fermions coupled to local dephasing and boundary drive and described within a Lindblad master equation. The model features an interplay between infinite temperature thermalization due to bulk dephasing and a nonequilibrium stationary state due to the boundary drive and dissipation. We revisit the linear and nonlinear transport properties of the model, featuring a crossover from ballistic to diffusive scaling, and compute the spectral and occupation properties encoded in the single-particle Green's functions, that we compute exactly using the Lindblad equations of motion in spite of the *interacting* nature of the dephasing term. We show that the distribution function in the bulk of the system becomes frequency independent and flat, consistent with infinite temperature thermalization, while near the boundaries it retains strong nonequilibrium features that reflect the continuous injection and depletion of particles due to driving and dissipation.

I. INTRODUCTION

Transport and thermalization are two fundamental phenomena that occur at the macroscopic scale. Their microscopic understanding has been the subject of a long standing effort both in the classical statistical mechanics context [1] as well as in the quantum domain [2]. One can generically distinguish two settings, depending on whether the system remains isolated from or interacts with an environment. In the former setup, many-body interactions play the key role in establishing the time scales for transport of conserved charges and thermalization, whereas in the latter the environment dissipation is responsible for the late time stationary state.

A specific instance that has attracted interest is the one of open Markovian systems [3], in which the system is intrinsically mixed and described by a master equation for the density matrix. Here the competition between unitary and dissipative couplings can lead to nonequilibrium phase transitions between phases with different transport properties.

In this context, finding a simple model which captures the key physical aspects of transport and thermalization while being computationally tractable for large system sizes is particularly important. An example that has attracted specific interest is the so-called dephasing model, describing a free fermionic lattice system coupled to a local Markovian environment described by a jump operator proportional to the density of particles. This model has been introduced in

Refs. [4,5] as a toy model for the emergence of diffusive behavior for a single-particle system. The spectral properties of the model in terms of the Liouvillian spectrum have been extensively discussed [6] as well as its transport properties [7–12] when the model is supplemented by a boundary Markovian driving. The pure dephasing model is furthermore exactly solvable [13,14], its Lindbladian spectrum being obtainable through Bethe ansatz techniques [14–16]. Recent works have discussed various extensions of this model [17].

In this paper we revisit the transport properties of the dephasing model with boundary drive, and connect them to the onset of thermalization as defined from the emergence of a fluctuation-dissipation theorem in the single-particle Green's functions. We show how these can be computed exactly using the Lindblad equations of motion, thus complementing previous results obtained through an unraveling of the master equation and a diagrammatic expansion in the Markovian noise [18,19]. We focus in particular on the crossover/transition as the system size is increased between infinite temperature thermalization due to the bulk dephasing and the onset of a nonequilibrium steady-state current at finite size due to the boundary drive. We investigate the role of the dephasing rate on this scenario, as well as of the deviation from the linear response regime as the strength of the drive is increased.

This paper is structured as follows. In Sec. II we introduce the model and the nonequilibrium protocol. In Sec. III we discuss the main quantities of interest, namely, the stationary current and the local Green's functions, and summarize the results on how to compute them within the Lindblad equation. In Sec. IV we present numerical results, first recalling the transport properties of the model and then discussing

---

*xturkesh@sissa.it
†On Leave from Institut de Physique Théorique, Université Paris Saclay, CNRS, CEA, F-91191 Gif-sur-Yvette, France.
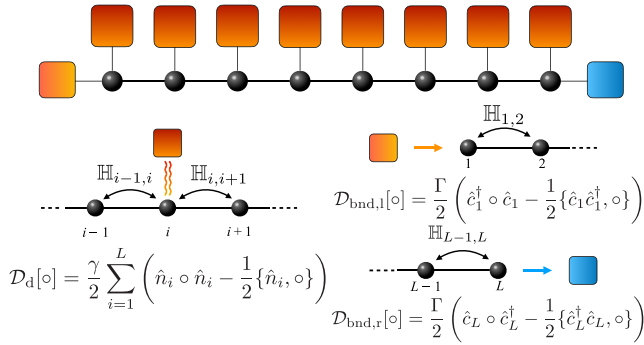
FIG. 1. The system when the boundary driving is open. The boundary terms inject absorb particles from the system. In addition, there is a uniform dephasing rate γ on each lattice site.

thermalization and effective temperature. We detail in the Appendices derivations of the various results used in the main text.

II. MODEL

We consider an open Markovian quantum system the density matrix of which evolves according to the Lindblad equation

$$\partial_t \hat{\rho}_t = \mathcal{L}\hat{\rho}_t = -i[\hat{H}, \hat{\rho}_t] + \mathcal{D}[\hat{\rho}_t]. \tag{1}$$

We denote with $[\hat{A}, \hat{B}](\{\hat{A}, \hat{B}\})$ the commutator (anticommutator) between $\hat{A}$ and $\hat{B}$. In Eq. (1), $\mathcal{H}$ is the Hamiltonian of the system, while the dissipation superoperator $\mathcal{D}$ collects the dissipation/dephasing terms. We set these objects in the following.

We consider a system of noninteracting spinless fermions defined in a one-dimensional chain of L sites with next-neighboring hopping rate J:

$$\hat{H} = \sum_{i=1}^{L-1} J(\hat{c}_i^\dagger \hat{c}_{i+1} + \text{H.c.}) + h\hat{c}_i^\dagger \hat{c}_i = \sum_{i,j=1}^{N} \hat{c}_i^\dagger \mathbb{H}_{i,j}\hat{c}_j,$$

$$\mathbb{H}_{i,j} = J\delta_{i,j+1} + J\delta_{i+1,j} + h\delta_{i,j}. \tag{2}$$

In Eq. (2) $\hat{c}_i$ ($\hat{c}_i^\dagger$) are the annihilation (creation) fermionic operators acting on the ith site, the one-particle Hamiltonian $\mathbb{H}$ is a $L \times L$ Hermitian and tridiagonal matrix, and we consider open boundary conditions.

We couple the left and right edge sites (Fig. 1), respectively, to a source and a sink. Specifically, particles are injected with a rate $\propto \Gamma$ on the first site, and are depleted with the same rate on the Lth site. These two terms are responsible for a direct current (DC) in the stationary state. In addition, on every lattice site we include a dephasing bath with rate $\propto \gamma$, which provides an energy relaxation channel. These three processes are collectively captured by the following dissipators:

$$\mathcal{D}[\circ] = \mathcal{D}_d[\circ] + \mathcal{D}_{bnd,l}[\circ] + \mathcal{D}_{bnd,r}[\circ], \tag{3}$$

$$\mathcal{D}_d[\circ] = \frac{\gamma}{2} \sum_{i=1}^{L} \left(\hat{n}_i \circ \hat{n}_i - \frac{1}{2}\{\hat{n}_i, \circ\} \right), \tag{4}$$

$$\mathcal{D}_{bnd,l}[\circ] = \frac{\Gamma}{2} \left(\hat{c}_1^\dagger \circ \hat{c}_1 - \frac{1}{2}\{\hat{c}_1\hat{c}_1^\dagger, \circ\} \right), \tag{5}$$

$$\mathcal{D}_{bnd,r}[\circ] = \frac{\Gamma}{2} \left(\hat{c}_L \circ \hat{c}_L^\dagger - \frac{1}{2}\{\hat{c}_L^\dagger\hat{c}_L, \circ\} \right). \tag{6}$$

Above, we introduced the fermion number $\hat{n}_i \equiv \hat{c}_i^\dagger \hat{c}_i$. Equation (4) is the dephasing contribution, Eq. (5) is the particle-injection contribution acting on the first site, while Eq. (6) is the particle-ejection contribution acting on the last site.

We emphasize that this model is not quadratic due to the dephasing processes, yet as we will discuss, it is simpler than a fully interacting many-body system while retaining some interesting nontrivial aspects. The boundary driving introduces a further source of translational invariance breaking (other than the open boundary condition), which manifests in the presence of a stationary current. (See however Appendix C for the translational invariant version of the model discussed in this paper.)

In the following, we are interested in characterizing the stationary state of the system obtained under the Markovian evolution (1). In particular, we will focus on the single-particle correlation functions at equal times, and on the single-particle Green's functions, from which physical quantities can be obtained such as the average current or the local density of states (DOS). In the next section, we introduce these quantities and discuss how to evaluate them exactly for our model.

III. OBSERVABLES

A. Equal-time correlation function and current

We introduce the single-particle correlation matrix C, with elements

$$C_{n,m}(t) = \langle \hat{c}_n \hat{c}_m^\dagger \rangle_t = \text{tr}[\rho(t)\hat{c}_n\hat{c}_m^\dagger]. \tag{7}$$

This function encodes the average particle density

$$n_m(t) \equiv \langle \hat{n}_m \rangle_t = \text{tr}[\rho(t)\hat{c}_m^\dagger \hat{c}_m] = 1 - C_{m,m}(t), \tag{8}$$

as well as the average current operator. We note in fact that both the Hamiltonian and the dephasing dissipator commute with the total particle number, and therefore allow us to define a conserved current which is then transported due to the boundary drive terms. This reads, from the continuity equation for the Hamiltonian part only [see Eq. (2)],

$$\hat{j}_m \equiv iJ(\hat{c}_{m-1}^\dagger \hat{c}_m - \hat{c}_m^\dagger \hat{c}_{m-1}),$$

$$j_m(t) \equiv \langle \hat{j}_m \rangle_t = 2J \, \text{Im} \, C_{m,m-1}(t). \tag{9}$$

Its dynamics can be obtained by the Lindblad equation Eq. (1), with dissipator Eq. (3), and using the cyclic property of the trace [3]. We have

$$\partial_t C_{m,n}(t) = -iJC_{m-1,n}(t) - iJC_{m+1,n}(t)$$
$$+ iJC_{m,n+1}(t) + iJC_{m,n-1}(t)$$
$$+ \Gamma\delta_{m,N}\delta_{n,N} - \gamma(1 - \delta_{m,n})C_{m,n}(t)$$
$$- \frac{\Gamma}{2}(\delta_{1,n} + \delta_{1,m} + \delta_{N,n} + \delta_{N,m})C_{m,n}(t). \tag{10}$$

Notice that here we imposed $C_{0,k}(t) = C_{k,N+1}(t) = 0$ at every time step in Eq. (10), as open boundary conditions apply.

Remarkably, despite the fact that the dephasing acts as a four-body interaction, the equation of motion for the two-point function is closed and can be exactly computed. In fact, for the system of interest, the k-point equal time correlation function presents a hierarchical structure, where the k-point equal time correlation function decouples from higher order ones [6], whereas the state is non-Gaussian [18] and highly entangled [20].

It is convenient to rephrase Eq. (10) in matrix form. The terms proportional to the imaginary unit i are due to the commutation with the Hamiltonian, which in the fermionic representation is completely specified by $\mathbb{H}$ [see Eq. (2)]. The remaining terms are related to the dissipation. We define the matrix $\mathbb{D}$, the elements of which are $\mathbb{D}_{m,k} = \delta_{m,k}(\gamma + \delta_{m,1}\Gamma + \delta_{m,N}\Gamma)/2$, and the matrix P, the elements of which are $P_{m,k}(t) = \delta_{m,k}(\gamma C_{m,m}(t) + \Gamma\delta_{m,N}\delta_{k,N}) \equiv \delta_{m,k}p_k(t)$. With these choices, and defining, we have

$$\partial_t C = -i[\mathbb{H}, C] - \{\mathbb{D}, C\} + P \equiv -i\mathbb{H}_{\text{eff}}C + iC\mathbb{H}_{\text{eff}}^{\dagger} + P. \tag{11}$$

In the last step, we defined the first-quantization non-Hermitian Hamiltonian. In fact, manipulating Eq. (1) we obtain the natural non-Hermitian Hamiltonian

$$\hat{H}_{\text{eff}} = \sum_{i,j=1}^{L} \hat{c}_i^{\dagger} \mathbb{H}_{\text{eff}} \hat{c}_j. \tag{12}$$

In the following we show that the spectral properties of the non-Hermitian Hamiltonian determine the stationary values of the particle density and current, and of the Green's function (Sec. III B).

Despite the fact that the simulation of the whole dynamics Eq. (11) is polynomial in resources, the stationary solution is obtained exactly by solving $\partial_t C = 0$. This is given by [21,22]

$$C(\infty) = \int_0^{\infty} d\tau e^{-i\mathbb{H}_{\text{eff}}\tau} P(\infty) e^{i\mathbb{H}_{\text{eff}}^{\dagger}\tau}. \tag{13}$$

This integral equation is simplified once the eigendecomposition of the matrix $\mathbb{H}_{\text{eff}}$ is considered (see Appendix A for a coordinate Bethe ansatz solution). Its non-Hermitian nature gives rise to inequivalent left and right eigenvectors: $\mathbb{H}_{\text{eff}} = \sum_p \lambda_p |\varphi^{\text{R}}(p)\rangle\langle\varphi^{\text{L}}(p)|$. We fix the ambiguity in the eigenvector by choosing them biorthonormal $\langle\varphi^{\text{L}}(q)|\varphi^{\text{R}}(p)\rangle = \delta_{p,q}$. In this way, the series expansion reduces to the trivial

$$e^{i\tau\mathbb{H}_{\text{eff}}} = \sum_{k=1}^{L} e^{i\tau\lambda_k}|\varphi^{\text{R}}(k)\rangle\langle\varphi^{\text{L}}(k)|. \tag{14}$$

Defining the components $\varphi_i^{\text{R/L}}(p)$, and performing the integral, Eq. (13) transposes to

$$C_{i,j}(\infty) = \Gamma\Theta_{i,j,L} + \gamma\sum_{k=1}^{L}\Theta_{i,j,k}C_{k,k}(\infty),$$

$$\Theta_{i,j,l} \equiv -\sum_{p,q=1}^{L}\frac{\varphi_i^{\text{R}}(p)[\varphi_l^{\text{L}}(p)]^*[\varphi_j^{\text{R}}(q)]^*\varphi_l^{\text{L}}(q)}{i\lambda_p - i\lambda_q^*}. \tag{15}$$

Solving this linear system we obtain both the density of particles $n_m(\infty)$ [see Eq. (8)] and the stationary current $j_m(\infty)$ [see Eq. (9)].

We point out that the knowledge of the full tensor Θ is not required to obtain n_m and j_m. In fact, the density profile requires $\mathcal{O}(N^2)$ terms, whereas the stationary current only $\mathcal{O}(1)$ as $j_i(\infty) \equiv j_\infty$ is flat.

The latter is a consequence of the generalized continuity equation in the present setup. We conclude this section by showing that the stationary current is indeed constant throughout the system.

In the nonequilibrium steady state (NESS) we have

$$0 = \frac{d}{dt}n_1$$
$$= i\langle[\hat{H}, \hat{c}_1^{\dagger}\hat{c}_1]\rangle_{\text{NESS}} + \text{tr}(\hat{c}_1^{\dagger}\hat{c}_1\mathcal{D}_{\text{bnd},1}[\rho_\infty]), \tag{16a}$$

$$0 = \frac{d}{dt}n_k = i\langle[\hat{H}, \hat{c}_k^{\dagger}\hat{c}_k]\rangle_{\text{NESS}}, \quad 2 \leqslant k \leqslant L-1, \tag{16b}$$

$$0 = \frac{d}{dt}n_L$$
$$= i\langle[\hat{H}, \hat{c}_L^{\dagger}\hat{c}_L]\rangle_{\text{NESS}} + \text{tr}(\hat{c}_L^{\dagger}\hat{c}_L\mathcal{D}_{\text{bnd,r}}[\rho_\infty]). \tag{16c}$$

All the other terms, not reported, are zero. In fact, the dephasing damps the evolution of all the off-diagonal correlation matrix elements $C_{m,n}$ ($m \neq n$), while it does not contribute to the equation of motion of the particle density.

From the bulk equation, after a simple manipulation, we find

$$j_k = j_{k+1}, \quad 2 \leqslant k \leqslant L-1. \tag{17}$$

Let us define

$$j_l \equiv \Gamma(1 - n_1), \tag{18}$$

$$j_r \equiv \Gamma n_L, \tag{19}$$

respectively, the current incoming/outgoing into/from the system. These contributions are those arising from $\mathcal{D}_{\text{bnd,l/r}}$ in Eqs. (16a) and (16c), respectively. Hence, we find

$$j_l = j_2, \quad j_r = j_L. \tag{20}$$

Since the stationary current is constant throughout the system, we define the stationary current by the value $j_\infty \equiv j_k$ for any k evaluated at the steady state.

B. Nonequilibrium Green's functions

A richer information on the structure of the stationary state of the Lindblad master equation can be extracted from the nonequilibrium Green's functions, which describe the excitations on top of the NESS [3,23,24]. We define in particular the retarded/advanced/Keldysh Green's functions $G^{R/A/K}(t)$

$$G_{m,n}^R(t) = -i\theta(t)\langle\{\hat{c}_m(t), \hat{c}_n^{\dagger}\}\rangle_{\text{NESS}}, \tag{21a}$$

$$G_{m,n}^A(t) = i\theta(-t)\langle\{\hat{c}_m(t), \hat{c}_n^{\dagger}\}\rangle_{\text{NESS}}, \tag{21b}$$

$$G_{m,n}^K(t) = -i\langle[\hat{c}_m(t), \hat{c}_n^{\dagger}]\rangle_{\text{NESS}}, \tag{21c}$$

and their Fourier transforms

$$G^{R/A/K}(\omega) = \int_{-\infty}^{\infty} dt e^{i\omega t} G^{R/A/K}(t). \tag{22}$$

Since the stationary state is time-translational invariant, we have

$$G^{R/A}(\omega) = G^{A/R\dagger}(\omega), \quad G^K(t) = -G^{K\dagger}(-t), \quad (23)$$

where the matrix notation is understood.

In the definition above the average over the NESS is defined as

$$\langle X \rangle_{\text{NESS}} \equiv \text{tr}(\hat{\rho}_\infty X), \quad (24)$$

while we have introduced the evolution of the operator $\hat{c}_m(t)$, which is given by the modified adjoint Lindbladian

$$\frac{d}{dt}\hat{c}_m(t) = \tilde{\mathcal{L}}^\dagger \hat{c}_m(t), \quad (25)$$

with $\mathcal{L}$ defined as

$$\tilde{\mathcal{L}}^\dagger(\circ) \equiv i[\hat{H}, \circ] + \mathcal{D}_{\text{d}}[\circ] + \tilde{\mathcal{D}}_{\text{bnd,l}}[\circ] + \tilde{\mathcal{D}}_{\text{bnd,r}}[\circ], \quad (26)$$

$$\tilde{\mathcal{D}}_{\text{bnd,l}}[\circ] = \Gamma\left(\eta\hat{c}_1 \circ \hat{c}_1^\dagger - \frac{1}{2}\{\hat{c}_1\hat{c}_1^\dagger, \circ\}\right), \quad (27)$$

$$\tilde{\mathcal{D}}_{\text{bnd,r}}[\circ] = \Gamma\left(\eta\hat{c}_L^\dagger \circ \hat{c}_L - \frac{1}{2}\{\hat{c}_L^\dagger\hat{c}_L, \circ\}\right). \quad (28)$$

In the above equation $\hat{H}$ and $\mathcal{D}_{\text{d}}$ are as in, respectively, Eqs. (2) and (4), while the phase $\eta = -1$ arises from the fermionic nature of the degrees of freedom. We refer to Refs. [25,26] for a first-principle derivation of Eq. (25).

Quite interestingly we can write exact equations of motions for those Green's functions. These read

$$\frac{d}{dt}G^R(t) = -i\delta(t)\mathbf{1} - i\mathbb{H}_{\text{eff}}G^R(t). \quad (29)$$

In frequency domain, the solutions of Eq. (29) for the retarded function and the advanced Green's function are given by

$$G^R(\omega) = (\omega - \mathbb{H}_{\text{eff}})^{-1}, \quad (30)$$

$$G^A(\omega) = [G^R(\omega)]^\dagger = (\omega - \mathbb{H}_{\text{eff}}^\dagger)^{-1}. \quad (31)$$

The tridiagonal and homogeneous nature of the matrix $\mathbb{H}_{\text{eff}}$ permits an exact solution for the component of $G^R(\omega)$ [27,28]. Introducing the auxiliary variable

$$\phi = \arccos\left[-\frac{1}{2}\left(\omega + i\frac{\gamma}{2}\right)\right], \quad \text{Re}(\phi) \in [0, \pi], \quad (32)$$

the matrix elements $G_{m,n}^R[\phi(\omega)]$ with $m \geqslant n$ are

$$G_{m,n}^R(\phi) = \frac{\sin[(L-m)\phi]}{\Delta(\phi)}\left(\frac{i\Gamma}{2}\sin(n\phi)\right.$$
$$\left. + \frac{\Gamma^2}{4J}\sin[(n-1)\phi]\right) + \frac{\sin[(L-m+1)\phi]}{\Delta(\phi)}$$
$$\times \left(\frac{i\Gamma}{2}\sin[(n-1)\phi] - J\sin(n\phi)\right), \quad (33)$$

$$\Delta(\phi) = \sin(\phi)\left(J^2\sin[(L+1)\phi]\right.$$
$$\left. - \frac{\Gamma^2}{4}\sin[(L-1)\phi] - iJ\Gamma\sin(L\phi)\right). \quad (34)$$

The remaining elements are given by transposition, as the retarded Green's function is symmetric: $G_{m,n}^R = G_{n,m}^R$. A comparison between numerical exact diagonalization and the

above analytic expressions is provided in Appendix D, as well as the scaling limit expression of these functions.

From the retarded Green function, we find the solution of the Keldysh equation of motion in frequency space. We have

$$G^K(\omega) = -2iG^R(\omega)\Lambda G^A(\omega), \quad (35)$$

$$\Lambda \equiv P(\infty) - \mathbb{D}, \quad (36)$$

with Λ the exact self-energy of the system, and $P(\infty)$ and $\mathbb{D}$ defined in Sec. III A. A derivation of this expression is given in Appendix B.

C. A relation between current and Green's functions for the driven-dephasing model

Using the equation of motions technique we can obtain an exact relation between the stationary current and the Green's functions for the driven-dephasing model. This generalizes recent results for a model without dephasing [29] analog to the Meir-Wingreen formula [30], obtained within the Keldysh path integral formulations [31].

We proceed as in Ref. [29] and evaluate the stationary current at the boundary. As previously argued, since in our setting the current is constant throughout the system, it is convenient to use (either) expression in Eq. (19) to relate the current to the $R/A/K$ Green's functions by means of the density.

From the definition Eq. (21), we have

$$n_m(\infty) = \langle \hat{c}_n^\dagger \hat{c}_m \rangle_{\text{NESS}}$$
$$= \frac{i}{2}\int \frac{d\omega}{2\pi}\left[G_{m,m}^R(\omega) - G_{m,m}^A(\omega) - G_{m,m}^K(\omega)\right]. \quad (37)$$

Using the sum rule, valid in the NESS,

$$\mathbf{1} = i\int \frac{d\omega}{2\pi}[G^R(\omega) - G^A(\omega)], \quad (38)$$

and $j_\infty = \Gamma(1 - n_1)$, we find after simple algebra [see also Eq. (B4)]

$$j_\infty = \Gamma \int \frac{d\omega}{2\pi}\langle 1|G^R(\omega)P(\infty)G^A(\omega)|1\rangle. \quad (39)$$

We conclude this section by remarking that, if the integral over frequency is formally performed, we recast the current reading of Eq. (15). In fact, from the eigendecomposition of $\mathbb{H}_{\text{eff}}$, and using

$$\int \frac{d\omega}{2\pi}\frac{1}{(\omega - \lambda_p)(\omega + \lambda_q)} = -\frac{1}{i\lambda_p - i\lambda_q^*}, \quad (40)$$

we recast

$$j_\infty = \Gamma\sum_k \Theta_{1,1,k}p_k, \quad (41)$$

which is obtained from Eqs. (39) and (19). The advantage of Eq. (39) over Eq. (15) lies in the direct physical interpretation of the Green's functions, which are furthermore relevant also for experimental setups.

D. Connection with Keldysh field theory and stochastic unraveling

The results reported above show that using Lindblad equations of motion one can compute exactly the single-particle Green's functions of the driven-dephasing model, despite the fact that the Lindbladian is not quadratic in the fermionic creation/annihilation operators. This implies that the Keldysh diagrammatics associated to the Lindblad master equation, while containing a dissipative interaction vertex due to the dephasing, admits a resummation in terms of a closed form self-energy for the single-particle Green's function. The resummability of the dephasing diagrammatics has been previously discussed by unraveling the Lindblad master equation into a stochastic quantum trajectory, first in Refs. [18,32] for an impurity problem and recently in Ref. [19] for a more general setting. In this picture in fact the noisy Hamiltonian would only feature quadratic terms in the fermion operators and one could compute exactly the Green's function for this problem, at least for a given realization of the stochastic process. Averaging over the (Markovian) noise would lead to a diagrammatic expansion, containing only noncrossing diagrams, which can be resummed in closed form [18,19,32]. In this respect our paper, which makes use of the Lindblad equation of motions rather than of a diagrammatic expansion in the noise, provides a complementary perspective on this resummability and extends the well-known results for the steady state and its static correlators [4,6,10] to the dynamical (Green's functions) case. Finally, we note that for a generic non-Markovian bath (or noise) the diagrammatic expansion would contain both crossing and noncrossing diagrams. Nevertheless one could still show that the results obtained within a Lindblad master equation are equivalent to a noncrossing approximation in the system-bath coupling (or noise) [33].

IV. RESULTS

In this section we discuss our results for the current and the Green's functions of the model. For simplicity we fix $J = 1$ in the following and study the properties of the system as a function of the dephasing γ and the strength of the drive Γ.

A. Transport: Current and density profile

We start by reviewing the transport properties of the system, which have been extensively discussed in the literature [2,7,9]. In the presence of a finite pump-loss boundary drive, a homogeneous stationary state with a finite current arises. We define the resistance $R_\infty = 1/j_\infty$. In our setting, the stationary current is given by [7]

$$j_\infty = \frac{4\Gamma}{\Gamma^2 + 4 + (L-1)\Gamma\gamma} \simeq D\frac{4}{L}, \quad D = 1/\gamma,$$

$$R_\infty = \frac{1}{2}\left(\frac{\Gamma}{2} + \frac{2}{\Gamma} + (L-1)\frac{\gamma}{2}\right) \simeq \frac{\gamma}{4}L. \quad (42)$$

Diffusive behavior is signaled by $R(L) \propto L$, as clearly shown in Fig. 2 (top panel). The existence of diffusion in the model without boundary drive can be established analytically by analyzing the spectral properties of the Lindbladian [4,5]. We note that the resistance shows a crossover from a ballistic to a
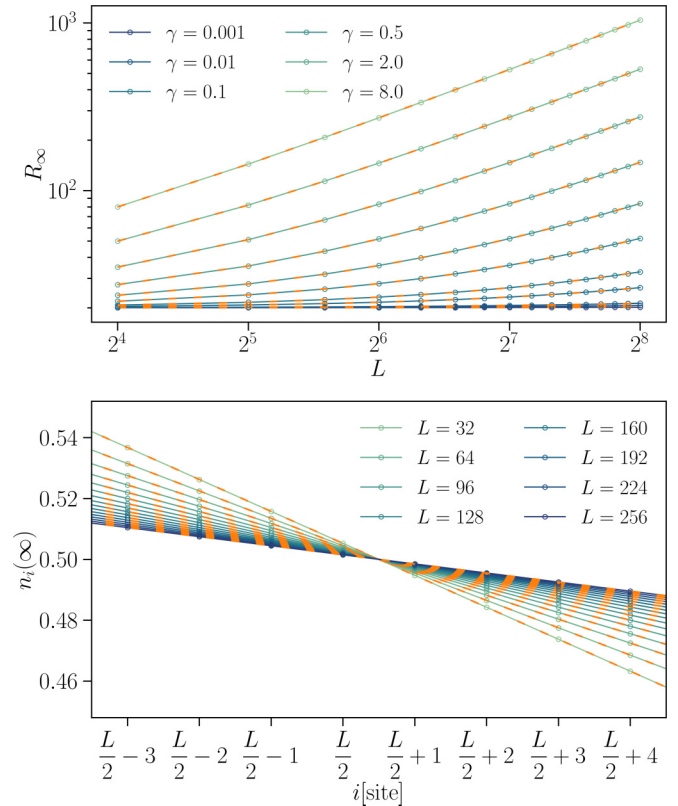

FIG. 2. Top: Resistance of the system vs system size L for different values of γ and $\Gamma = 0.1$. At small values of γ, the system clearly displays a crossover between a ballistic and a diffusive regime. The dashed orange lines correspond to Eq. (42). Bottom: Density profile $n_i(\infty)$ for various system sizes L for $\gamma = 0.5$ and $\Gamma = 0.1$. The slope around $i = L/2$ is $\propto 1/L$. The dashed orange lines correspond to Eq. (43).

a diffusive scaling [6], as a function of the dephasing rate γ as we show in Fig. 2. A diffusive current should correspond to the onset of a stationary state density profile at site i of the form [7]

$$\frac{\Delta n_i}{\Delta i} = \frac{\gamma\Gamma}{\Gamma^2 + 1 + (L-1)\gamma\Gamma} \xrightarrow{L \gg 1} \frac{1}{L}. \quad (43)$$

In the previous equation we have considered the scaling limit, where Fick's law is recovered. We see that the density drops near the boundary, while in the bulk the system in the thermodynamic limit approaches a constant density profile with $n \to 1/2$, consistent with an infinite temperature thermalization as we will discuss in more detail below.

We now discuss the dependence of the stationary current j_∞ from the strength of the drive Γ and the dephasing rate γ. As we show in the top panel of Fig. 3, the current is linear at small Γ, reaches a maximum at Γ^*, and then starts to decrease, eventually going to zero as $1/\Gamma$ for $\Gamma \gg 1$. This indicates that when the drive is much larger than the single-particle bandwidth resonance responsible for coherent transport is not efficiently established and the current decreases. A finite dephasing rate does not change the linear regime while it strongly reduces the maximum current which can be sustained by the system. From Eq. (42) we obtain that j_∞^*,
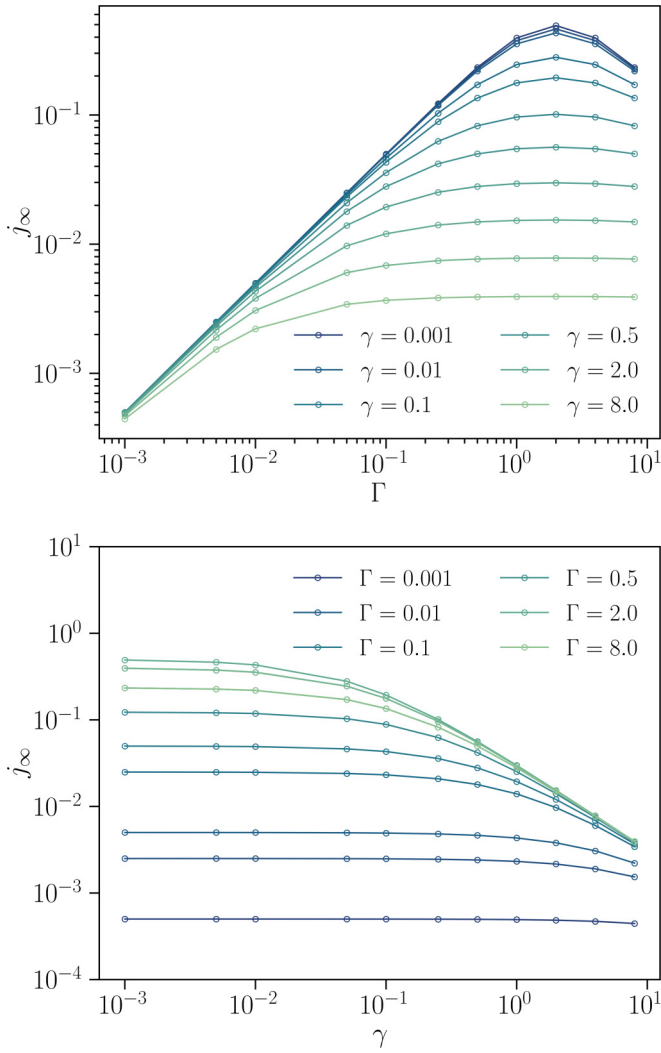
FIG. 3. Stationary current j_∞ as a function of the drive strength Γ (top panel) and dephasing rate γ (bottom panel) for a fixed system size $L = 256$. We see that the linear regime $j_\infty \sim \Gamma$ is independent of the dephasing rate while the maximum current is strongly suppressed by increasing γ, which plays a role similar to inelastic many-body interactions.

corresponding to the current at the optimal coupling Γ^*, scales as $j_\infty^* \sim 1/\gamma L$. In the bottom panel we show the current as a function of the dephasing rate from which again we can see how the linear regime is almost unaffected by the scattering while at stronger drive the current decreases with γ and eventually vanishes as $1/\gamma$ in accordance with Eq. (42). Overall these results confirm the physical picture that a finite dephasing rate is detrimental to coherent transport, playing a similar role as inelastic scattering due to many-body interactions or heating due to finite temperature.

B. Local density of states and distribution function

We now discuss the Green's functions of the model. We start with the retarded Green's function at site n, the imaginary part of which

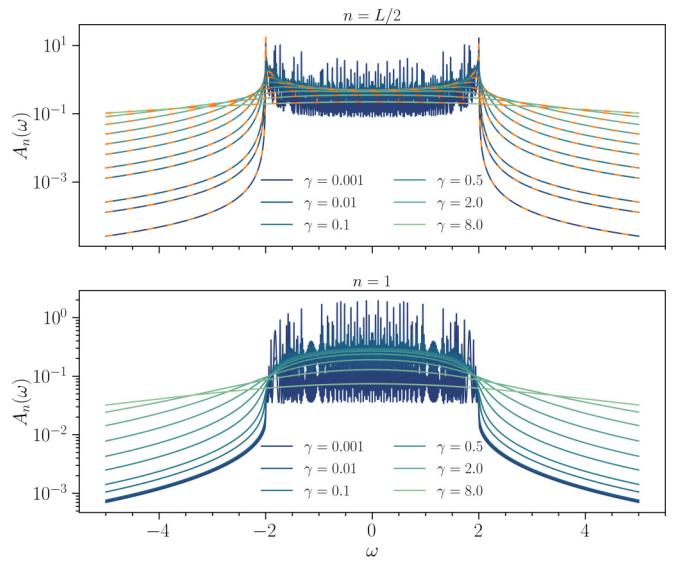$$A_n(\omega) = -\frac{1}{\pi} \text{Im} G_{n,n}^R(\omega) \qquad (44)$$

FIG. 4. Local density of states. Top: $A_n(\omega)$ at the center of the chain $n = L/2$ as a function of frequency, compared with the translational invariant result Eq. (46) (dashed orange lines), for different values of the dephasing. Bottom: Local DOS $A_n(\omega)$ at the boundary of the chain $n = 1$ as a function of frequency and different values of the dephasing rate.

describes the local DOS of the system. This can be obtained directly from the results of Sec. III B [see Eq. (33)].

Before discussing the case $\gamma > 0$, we briefly comment on the $\gamma = 0$ case. In this situation, Eq. (33) reduces to the ballistic formula, and the results in Ref. [29] are recovered.

Turning on the dephasing in the system has important consequences. The auxiliary variable $\phi = \arccos[-\frac{1}{2}(\omega + i\frac{\gamma}{2})]$ acquires an imaginary part which suppresses the matrix elements $G_{m,n}^R$. Quantitatively, starting from Eq. (33) we obtain the scaling limit $L \gg 1$:

$$G_{m,n}^R(\phi) = -e^{im\phi} \frac{2i \sin(n\phi) + \Gamma \sin[(n-1)\phi]}{\sin(\phi)(2i + e^{i\phi}\Gamma)}. \qquad (45)$$

The above expression is exact for the thermodynamic limit of any component of the retarded function, provided $\gamma > 0$. For a site in the bulk $n \sim L/2 \gg 1$ the above expression simplifies to

$$G_{n,n}^R(\phi) = \frac{-i}{\sqrt{4 - (\omega + i\gamma/2)^2}} \qquad (46)$$

which as expected is independent both from the site index and from the boundary drive Γ. Importantly, Eq. (46) matches the translational invariant result (Appendix C; see Appendix D for a comparison).

In Fig. 4 we plot the local DOS in the middle of the chain and at the boundary (respectively, top and bottom panels) for different values of γ. In the bulk we see for small dephasing two sharp edges around $\omega = \pm 2$ which are further smeared out by increasing the dephasing rate. We can understand this result by noticing that in the absence of any boundary drive the system is translationally invariant (see Appendix C) and the local DOS displays the characteristic square-root singularities at the edge of the single-particle bandwidth smeared by a Lorentzian weight which is due to the dephasing and that

results in additional tails at large frequencies. As expected therefore the behavior in the bulk is essentially independent of the value of the boundary drive, at least for large enough system sizes. Close to the boundary on the other hand we expect a much stronger dependence from the drive strength, as we show in Appendix D. In the bottom panel of Fig. 4 we plot the boundary local DOS for different values of the dephasing rate, showing that while the single-particle band edges are still visible for small γ there are no signatures of the sharp singularities seen in the bulk. For large values of γ instead the bulk and the boundary DOS are essentially the same, corresponding to very broad linewidth.

We see that despite the *interacting* nature of the dephasing rate, which enters the Lindblad master equation with a quadratic jump operator, the scale γ plays essentially the role of a dissipative width and does not induce any frequency dependent self-energy corrections for the momentum resolved Green's function, while the local DOS has a sizable spectral redistribution from low to high frequency due to the dephasing.

A complementary perspective on the competition between dephasing and boundary terms is provided by the local Keldysh Green's function $G_n^K(\omega)$, defined in Eq. (21c), which describes the occupation of the single-particle excitations on top of the stationary state. It is convenient to parametrize it through the distribution function, which is defined in analogy with the thermal equilibrium case. In fact, if the system was in true thermal equilibrium, the quantum fluctuation-dissipation theorem (FDT) would constrain the Keldysh and the retarded components to obey the relation [31]

$$\frac{G_{n,n}^K(\omega)}{-2\pi i A_{n,n}(\omega)} \equiv F^{\mathrm{eq}}(\omega) = \tanh\left(\frac{\omega}{2T}\right) \qquad (47)$$

where T is the system temperature. At low frequency or high temperatures $\omega \ll T$, one has $F^{\mathrm{eq}}(\omega) \sim \omega/T$. In a nonequilibrium system, in contrast, there is no well-defined temperature and the FDT does not hold in general. Nonetheless, it is useful to use the left-hand side of the FDT in Eq. (47) to *define* an effective distribution function:

$$F_n^{\mathrm{neq}}(\omega) = \frac{iG_{n,n}^K(\omega)}{2\pi A_{n,n}(\omega)}. \qquad (48)$$

We plot the nonequilibrium distribution $F_n^{\mathrm{neq}}(\omega)$ in Fig. 5 for different lattice sites (corresponding to different lines in each panel) and we compare it to the retarded and Keldysh Green's functions (see central and bottom panels). We see that the distribution function close to the boundaries (top and bottom lines) is strongly frequency dependent and highly athermal. In particular $F_n^{\mathrm{neq}}(\omega)$ is an even function of frequency, unlike the thermal result in Eq. (47), and odd under spatial inversion around the center of the lattice. This feature arises directly from the Keldysh Green's function (see bottom panel of Fig. 5) while the retarded Green's function is symmetric under inversion (central panel), and reflects the symmetry between injection and depletion at the boundaries. In fact we can see from Eq. (37) that the frequency integral over the Keldysh Green's function quantifies the deviation of the local occupation from the bulk value $n = 1/2$. Therefore near the boundary where injection (depletion) occurs we ex-
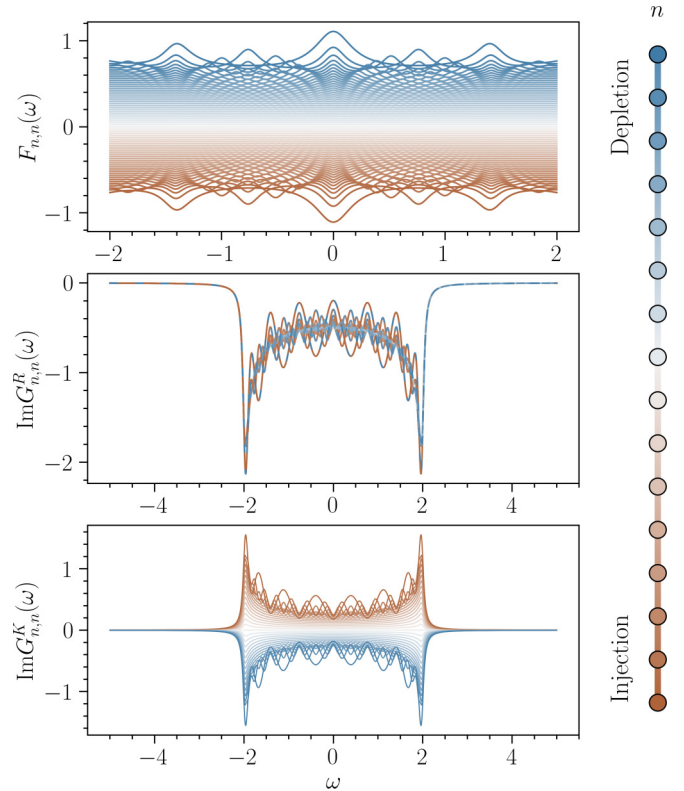

FIG. 5. For all panels we fix $L = 256$, $\gamma = 0.1$, and $\Gamma = 0.1$. Top: Distribution function at different sites in the chain. Center: Imaginary part of the retarded function. Bottom: Imaginary part of the Keldysh Green's function.

pect an increase (decrease) of density and correspondingly a Keldysh Green's function which is of positive (negative) sign. Alternatively, we can parametrize the distribution function in terms of an effective Fermi function $F_n^{\mathrm{neq}}(\omega) = 1 - 2f_n(\omega)$ from which we conclude that positive (negative) values of the distribution function correspond to an increased (decreased) occupancy of the Fermi function. Upon approaching the bulk of the system, on the other hand, we see that the distribution function becomes flatter in frequency and its value approaches zero, a signature of the onset of bulk thermalization to infinite temperature. To further discuss this point we introduce a frequency-dependent inverse effective temperature [34–39]:

$$\beta_n(\omega) = \frac{1}{2\omega} \mathrm{arctanh}\left[F_n^{\mathrm{neq}}(\omega)\right]. \qquad (49)$$

We plot the inverse effective temperature in Fig. 6 at the bulk and at the boundaries for different system sizes L. We see that in the bulk of the system ($n = L/2$, top panel) $\beta_n(\omega)$ shows small oscillations for frequencies within the single-particle bandwidth, which are rapidly damped out upon increasing L leaving a constant value which approaches zero in the thermodynamic limit, with a uniform scaling $1/L$ that comes from the Keldysh Green's function. At the boundary instead the effective temperature depends on frequency, as we show in the bottom panel of Fig. 6. In particular we note that for frequencies within the single-particle bandwidth $\beta_n(\omega)$ is smaller in absolute value, corresponding to an increased heating and
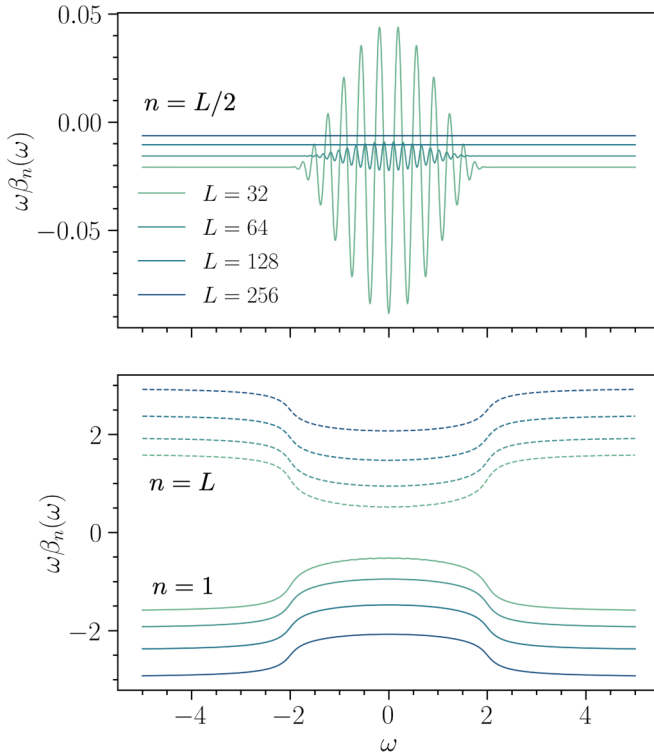
FIG. 6. Inverse effective temperature $\omega\beta_n(\omega)$, defined as in Eq. (49) of the main text, at $\Gamma = 1/4$ and $\gamma = 1/4$ in the bulk (top) and in the boundaries (bottom), for different system sizes.

thermalization due to resonant single-particle processes as compared to the high frequency regions.

V. CONCLUSION

In this paper we have studied transport and thermalization in a simple model of noninteracting one-dimensional spinless fermions subject to local dephasing and boundary drive. Within the framework of the Lindblad master equation of open quantum systems we have shown that the problem can be exactly solved both for what concerns single-particle static correlation functions, giving access to the current in the nonequilibrium steady state, as well as for the single-particle Green's functions describing excitations on top of the stationary state. In particular we have obtained a closed form expression for the local retarded Green's function, from which the Keldysh component can be readily obtained, and a relation between the stationary current and the single-particle Green's functions of the system, similar to the famous Meir-Wingreen formula, which generalizes to the dephasing case a recent result obtained within Keldysh techniques.

Using this framework we have revisited the transport properties of the system, featuring a well-studied crossover between ballistic and diffusive behavior in the scaling of the current versus system size. We have discussed how a finite dephasing rate introduces a resistivity growing with system size and a density profile decreasing linearly in the bulk. Going beyond the linear transport regime we have further shown that the dephasing strongly reduces the maximum current which can flow through the system at a given system size.

Furthermore we discussed the spectral properties of the model as encoded in the local density of states and in the single-particle distribution function. We have shown that the former in the bulk can be understood by considering the homogeneous translationally invariant case, where dephasing plays essentially the role of an additional linewidth broadening the edge singularities of the single-particle DOS, while the boundary DOS features a much broader linewidth due to the additional driving term. Finally we have shown that the distribution function at the boundary is highly nonequilibrated, reflecting the local injection and depletion of particles, while approaching the bulk site it becomes flatter in frequency consistent with the onset of infinite temperature thermalization.

We conclude by noticing that the above analysis has been performed for a translationally invariant system (boundary terms aside), however the Lindblad equation of motion technique used here can be naturally extended to disordered systems where one expects anomalous transport behavior. Results along these lines will be reported elsewhere [40].

APPENDIX A: SPECTRUM OF THE NON-HERMITIAN HAMILTONIAN

In this section we briefly review the diagonalization of the non-Hermitian Hamiltonian $\mathbb{H}_{\text{eff}}$ by means of the coordinate Bethe ansatz. A comprehensive analysis on the existence of the solutions and on their derivation was given in Refs. [27,28]. For simplicity we discuss the case of the right eigenvector, and fix $J = 1$. Using the Bethe ansatz $\varphi_l(k) = A_k e^{i\theta_k l} + B_k e^{-i\theta_k l}$, the eigensystem

$$\mathbb{H}_{\text{eff}}|\varphi(k)\rangle = \lambda_k|\varphi(k)\rangle \tag{A1}$$

reduces to

$$A_k = -\frac{2i + \Gamma e^{-i\theta_k}}{2i + \Gamma e^{i\theta_k}} B_k, \tag{A2}$$

$$\lambda_k = -i\frac{\gamma}{2} + 2\cos\theta_k, \tag{A3}$$

$$0 = \sin[(L+1)\theta_k] - \frac{\Gamma^2}{4}\sin[(L-1)\theta_k] - i\Gamma\sin(L\theta). \tag{A4}$$

The quantization condition Eq. (A4) fixes the values of $\theta_k \in [0, \pi[$, and hence the eigenvalues λ_k. However, for generic values of Γ, we lack a closed form expression of the complex angles θ_k, which need to be computed analytically. Inserting the obtained expressions for θ in the definition of $|\varphi(k)\rangle$ and using Eq. (A2), we obtain the right eigenvector. Similarly the left eigenvector can be obtained through symmetry

argument on $\mathbb{H}_{\text{eff}}$. The norm (free coefficient B_k) is fixed by the biorthonormal condition.

APPENDIX B: DERIVATION OF THE KELDYSH GREEN'S FUNCTION

The equation of motion of the Keldysh Green's function is

$$G^K(t) = \begin{cases} e^{tT} G^K(0), & t > 0, \\ G^K(0) e^{-tT^\dagger}, & t < 0. \end{cases} \quad (B1)$$

In frequency domain we have

$$\begin{aligned} G^K(\omega) &= \int_{-\infty}^{\infty} dt\, e^{i\omega t} G^K(t) \\ &= \int_0^{\infty} dt\, e^{i\omega t + tT} G^K(0) + \int_{-\infty}^0 dt\, G^K(0) e^{i\omega t - tT^\dagger} \\ &= \frac{-1}{i(\omega - iT)} G^K(0) + G^K(0) \frac{1}{i(\omega + iT^\dagger)} \\ &= \frac{i}{\omega - iT} G^K(0) - G^K(0) \frac{i}{\omega + iT^\dagger}. \quad (B2) \end{aligned}$$

From the definition Eq. (21c), we read $G^K(0) = i - 2iC(\infty)$. Hence

$$\begin{aligned} G^K(\omega) &= -G^R(\omega) + G^A(\omega) \\ &\quad + 2G^R(\omega)[iC(\infty)T^\dagger + iTC(\infty)] G^A(\omega) \quad (B3) \\ &= -G^R(\omega) + G^A(\omega) - 2iG^R(\omega) P(\infty) G^A(\omega). \quad (B4) \end{aligned}$$

The final expression Eq. (36) is recovered once the difference between retarded and advanced Green functions is performed:

$$-G^R(\omega) + G^A(\omega) = 2iG^R(\omega) \mathbb{D} G^A(\omega). \quad (B5)$$

En passant, we note expression Eq. (B4) is useful in deriving the Landauer formula Eq. (39).

APPENDIX C: TRANSLATIONAL INVARIANCE PURE DEPHASING MODEL

If we disregard the boundary drive, and close the chain to enforce periodic boundary conditions, the system becomes translationally invariant. In this situation, the correlation functions depend only on the distance, and the equations of motion for the Green's functions can be solved in Fourier space. We define the momentum resolved Green's functions

$$G^{R/A/K}(q, \omega) = \sum_n e^{-inq} G_n^{R/A/K}(\omega) \quad (C1)$$

where we have introduced the translationally invariant Green's functions $G_{m,n}^{R/A/K}(\omega) = G_{m-n}^{R/A/K}(\omega)$. The retarded component takes the simple form

$$G^R(q, \omega) = \frac{1}{\omega - \varepsilon(q) - i\gamma/2} \quad (C2)$$

which gives a spectral function in the form of a Lorentzian centered around the bare dispersion $\varepsilon(q) = -2J \cos(2\pi q/N)$. The local density of states becomes site independent and equal to

$$A(\omega) = -\frac{1}{\pi} \sum_q \frac{2\gamma}{4[\omega - \varepsilon(q)]^2 + \gamma^2}. \quad (C3)$$
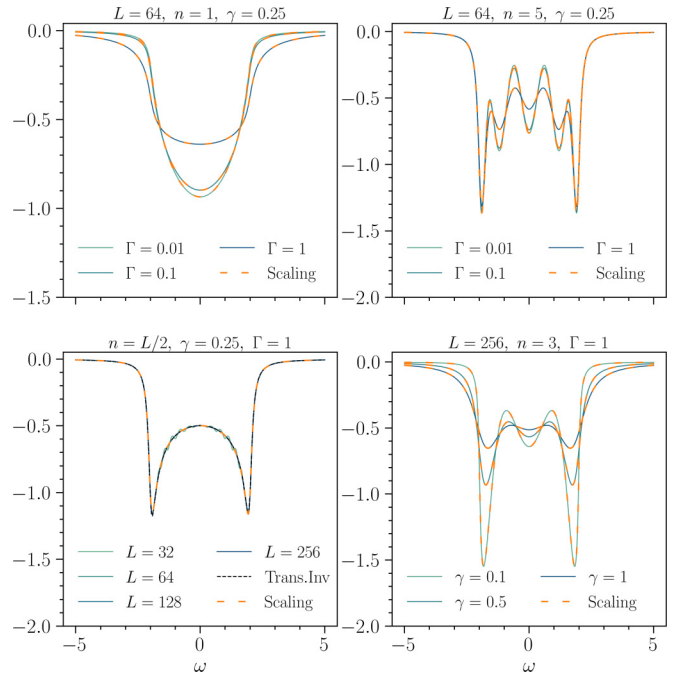

FIG. 7. Comparison between Eq. (33) and the exact diagonalization results from Eq. (38). The dashed orange lines are Eq. (33), whereas the dotted black line is the translational invariant limit Eq. (C5).

We introduce the density of states of the one-dimensional tight binding chain:

$$\begin{aligned} D(\varepsilon) &= \sum_q \delta[\varepsilon - \varepsilon(q)] = \int_{-\pi}^{\pi} dq\, \delta[\varepsilon + 2J \cos(q)] \\ &= \theta(4J - \varepsilon^2) \frac{1}{\sqrt{4J - \varepsilon^2}}, \quad (C4) \end{aligned}$$

which is centered around $\varepsilon = 0$ with a bandwidth of $4J$ and sharp edges. The smear by dephasing results in states in the tails outside of the kinetic bandwidth. With the above definition the final result for the local density of state is

$$\begin{aligned} A(\omega) &= -\frac{1}{\pi} \int d\varepsilon\, D(\varepsilon) \frac{2\gamma}{4(\omega - \varepsilon)^2 + \gamma^2} \\ &= -\frac{2\gamma}{\pi} \int_{-2J}^{2J} d\varepsilon \frac{1}{\sqrt{4J - \varepsilon^2}} \frac{1}{4(\omega - \varepsilon)^2 + \gamma^2}. \quad (C5) \end{aligned}$$

The Keldysh Green's function on the other hand can be obtained from Eq. (36). Because of translational symmetry, $\Lambda = \gamma(1 - 2n)/2$ is proportional to the identity. Hence, the Keldysh Green's function in Fourier space reads

$$G^K(q, \omega) = -i\gamma(1 - 2n) G^R(q, \omega) G^A(q, \omega), \quad (C6)$$

and it is therefore identically zero, since $n = 1/2$, which is again consistent with infinite temperature thermalization.

APPENDIX D: NUMERICAL BENCHMARKS

We benchmark the exact retarded Green's function Eq. (33) with the results from exact diagonalization and the values of the translationally invariant system. As in Sec. IV, we

fix $J = 1$. The comparison is given in Fig. 7. We note that the formula matches exactly the results for different sites, different parameters γ and Γ, and the translationally invariant limit in the bulk.

[1] L. Bertini, A. De Sole, D. Gabrielli, G. Jona-Lasinio, and C. Landim, Macroscopic fluctuation theory, Rev. Mod. Phys. **87**, 593 (2015).

[2] B. Bertini, F. Heidrich-Meisner, C. Karrasch, T. Prosen, R. Steinigeweg, and M. Žnidarič, Finite-temperature transport in one-dimensional quantum lattice models, Rev. Mod. Phys. **93**, 025003 (2021).

[3] H. P. Breuer and F. Petruccione, *The Theory of Open Quantum Systems*, 1st ed. (Oxford University, New York, 2007).

[4] M. Esposito and P. Gaspard, Exactly solvable model of quantum diffusion, J. Stat. Phys. **121**, 463 (2005).

[5] M. Esposito and P. Gaspard, Emergence of diffusion in finite quantum systems, Phys. Rev. B **71**, 214302 (2005).

[6] V. Eisler, Crossover between ballistic and diffusive transport: The quantum exclusion process, J. Stat. Mech.: Theory Exp. (2011) P06007.

[7] M. Žnidarič, Exact solution for a diffusive nonequilibrium steady state of an open quantum chain, J. Stat. Mech. (2010) L05002.

[8] M. Žnidarič, B. Žunkovič, and T. Prosen, Transport properties of a boundary-driven one-dimensional gas of spinless fermions, Phys. Rev. E **84**, 051115 (2011).

[9] M. Žnidarič, A matrix product solution for a nonequilibrium steady state of an XX chain, J. Phys. A: Math. Theor. **43**, 415004 (2010).

[10] M. Žnidarič, Solvable quantum nonequilibrium model exhibiting a phase transition and a matrix product representation, Phys. Rev. E **83**, 011108 (2011).

[11] M. Žnidarič and M. Horvat, Transport in a disordered tight-binding chain with dephasing, Eur. Phys. J. B **86**, 67 (2013).

[12] M. Žnidarič, A. Scardicchio, and V. K. Varma, Diffusive and Subdiffusive Spin Transport in the Ergodic Phase of a Many-Body Localizable System, Phys. Rev. Lett. **117**, 040601 (2016).

[13] M. V. Medvedyeva, F. H. L. Essler, and T. Prosen, Exact Bethe Ansatz Spectrum of a Tight-Binding Chain with Dephasing Noise, Phys. Rev. Lett. **117**, 137202 (2016).

[14] A. A. Ziolkowska and F. H. Essler, Yang-Baxter integrable Lindblad equations, Sci. Post Phys. **8**, 44 (2020).

[15] F. H. L. Essler and L. Piroli, Integrability of one-dimensional Lindbladians from operator-space fragmentation, Phys. Rev. E **102**, 062210 (2020).

[16] B. Buca, C. Booker, M. Medenjak, and D. Jaksch, Dissipative bethe ansatz: Exact solutions of quantum many-body dynamics under loss, arXiv:2004.05955.

[17] A. Bastianello, J. De Nardis, and A. De Luca, Generalized hydrodynamics with dephasing noise, Phys. Rev. B **102**, 161110(R) (2020).

[18] P. E. Dolgirev, J. Marino, D. Sels, and E. Demler, Non-Gaussian correlations imprinted by local dephasing in fermionic wires, Phys. Rev. B **102**, 100301(R) (2020).

[19] T. Jin, J. S. Ferreira, M. Filippone, and T. Giamarchi, Exact description of quantum stochastic models as quantum resistors, arXiv:2106.14765.

[20] V. Alba and F. Carollo, Spreading of correlations in Markovian open quantum systems, Phys. Rev. B **103**, L020302 (2021).

[21] V. K. Varma, C. de Mulatier, and M. Žnidarič, Fractality in nonequilibrium steady states of quasiperiodic systems, Phys. Rev. E **96**, 032130 (2017).

[22] S. R. Taylor and A. Scardicchio, Subdiffusion in a one-dimensional anderson insulator with random dephasing: Finite-size scaling, Griffiths effects, and possible implications for many-body localization, Phys. Rev. B **103**, 184202 (2021).

[23] A. Dorda, M. Nuss, W. von der Linden, and E. Arrigoni, Auxiliary master equation approach to nonequilibrium correlated impurities, Phys. Rev. B **89**, 165105 (2014).

[24] O. Scarlatella, A. A. Clerk, and M. Schiro, Spectral functions and negative density of states of a driven-dissipative nonlinear quantum resonator, New J. Phys. **21**, 043040 (2019).

[25] F. Schwarz, M. Goldstein, A. Dorda, E. Arrigoni, A. Weichselbaum, and J. von Delft, Lindblad-driven discretized leads for nonequilibrium steady-state transport in quantum impurity models: Recovering the continuum limit, Phys. Rev. B **94**, 155142 (2016).

[26] R. Citro and F. Mancini, *Out-of-Equilibrium Physics of Correlated Electron Systems*, Springer Series in Solid-State Sciences (Springer, New York, 2018).

[27] W.-C. Yueh and S. S. Cheng, Explicit eigenvalues and inverses of several toeplitz matrices, Anziam J. **48**, 73 (2006).

[28] W.-C. Yueh and S. S. Cheng, Explicit eigenvalues and inverses of tridiagonal Toeplitz matrices with four perturbed corners, Anziam J. **49**, 361 (2008).

[29] T. Jin, M. Filippone, and T. Giamarchi, Generic transport formula for a system driven by Markovian reservoirs, Phys. Rev. B **102**, 205131 (2020).

[30] Y. Meir and N. S. Wingreen, Landauer Formula for the Current Through an Interacting Electron Region, Phys. Rev. Lett. **68**, 2512 (1992).

[31] A. Kamenev, *Field Theory of Non-Equilibrium Systems* (Cambridge University, Cambridge, England, 2011).

[32] W. Berdanier, J. Marino, and E. Altman, Universal Dynamics of Stochastically Driven Quantum Impurities, Phys. Rev. Lett. **123**, 230604 (2019).

[33] O. Scarlatella and M. Schiro, Non-crossing dynamical maps for open quantum systems, arXiv:2107.05553.

[34] A. Mitra, S. Takei, Y. B. Kim, and A. J. Millis, Nonequilibrium Quantum Criticality in Open Electronic Systems, Phys. Rev. Lett. **97**, 236808 (2006).

[35] A. A. Clerk, M. H. Devoret, S. M. Girvin, F. Marquardt, and R. J. Schoelkopf, Introduction to quantum noise, measurement, and amplification, Rev. Mod. Phys. **82**, 1155 (2010).

[36] L. Foini, L. F. Cugliandolo, and A. Gambassi, Fluctuation-dissipation relations and critical quenches in the transverse field Ising chain, Phys. Rev. B **84**, 212404 (2011).

[37] E. G. Dalla Torre, E. Demler, T. Giamarchi, and E. Altman, Dynamics and universality in noise-driven dissipative systems, Phys. Rev. B **85**, 184302 (2012).

[38] M. Schiró and A. Mitra, Transient Orthogonality Catastrophe in a Time-Dependent Nonequilibrium Environment, Phys. Rev. Lett. **112**, 246401 (2014).

[39] L. M. Sieberer, M. Buchhold, and S. Diehl, Keldysh field theory for driven open quantum systems, Rep. Prog. Phys. **79**, 096001 (2016).

[40] X. Turkeshi *et al.* (unpublished).